JOURNAL OF MATERIALS SCIENCE 20 (1985) 3277 – 3282

Structural and optical properties of Zn_3P_2 thin films*

V. J. RAO, MADHURI V. SALVI, V. SAMUEL, A. P. B. SINHA
Physical Chemistry Division, National Chemical Laboratory, Poona 411 008, India

Conditions have been developed for the deposition of a stoichiometric thin film of zinc phosphide (Zn_3P_2) using electron beam evaporation. Structural properties of as-deposited and annealed thin films of zinc phosphide have been studied using electron and X-ray diffraction. The as-deposited film is non-crystalline, structural ordering starts on annealing at 200° C and the film becomes crystalline at 300° C with the structure matching that of the bulk material. Optical absorption has been investigated over the range 1 to 3 eV with emphasis on the region of interband absorption. The thin film absorption edge is found to be exponential for lower values of absorption coefficient. Analysis of thin film data showed that Zn_3P_2 is a direct-band-gap material. On annealing there is a shift in the band edge towards higher energy.

1. Introduction

Zinc phosphide has emerged as a promising new low-cost, high-efficiency photovoltaic material because of its many desirable characteristics [1–6]. Since it is a direct-band-gap material, thin films are adequate to absorb almost the entire amount of solar energy. There is therefore a lot of interest in developing methods for growing thin films of this material. Since this is a compound semiconductor, there have been difficulties in getting stoichiometric films. We have therefore investigated several methods and optimized conditions to get the desired films. With this end in view it has been necessary to characterize our films by measuring the important properties, namely the structural properties and optical absorption. The purpose of this work is also to obtain further information on the band structure of Zn_3P_2 by measuring optical absorption of thin films in the high absorption region up to photon energies of 3 to 3.5 eV. This is necessary because semiconducting Zn_3P_2 has not been investigated thoroughly in thin film form and its energy band structure is not very well known at present.

2. Experimental details

Zn_3P_2 was directly synthesized from its elements by reaction in an evacuated silica ampoule [7, 8]. Stoichiometric quantities of 99.999% zinc and 99.999% red phosphorus were slowly heated at 850° C for 24 h. The polycrystalline ingot thus obtained was used to grow a single crystal by a perforated capsule technique [9]. The single crystal furnished the starting material for deposition of thin films on glass and NaCl substrates.

Thin film deposition was done using a Hind Hivac electron beam evaporator. Source-to-substrate distance was about 10 to 12 cm and the background pressure 2×10^{-5} torr, during evaporation. The substrates were kept at room temperature. The polycrystalline ingot, the single crystal and the thin films were analysed by X-ray diffraction (XRD). The lattice parameters as found from the single-crystal data are $a = 0.8095$ nm and $c = 1.195$ nm. Film thickness was estimated ellipsometrically using a Gaertner Ellipsometer L119X and the thickness of the films was found to vary from 30 to 50 nm. Optical absorption measurements were per-

---

*NCL Communication No. 3571.

0022–2461/85 $03.00 + .12

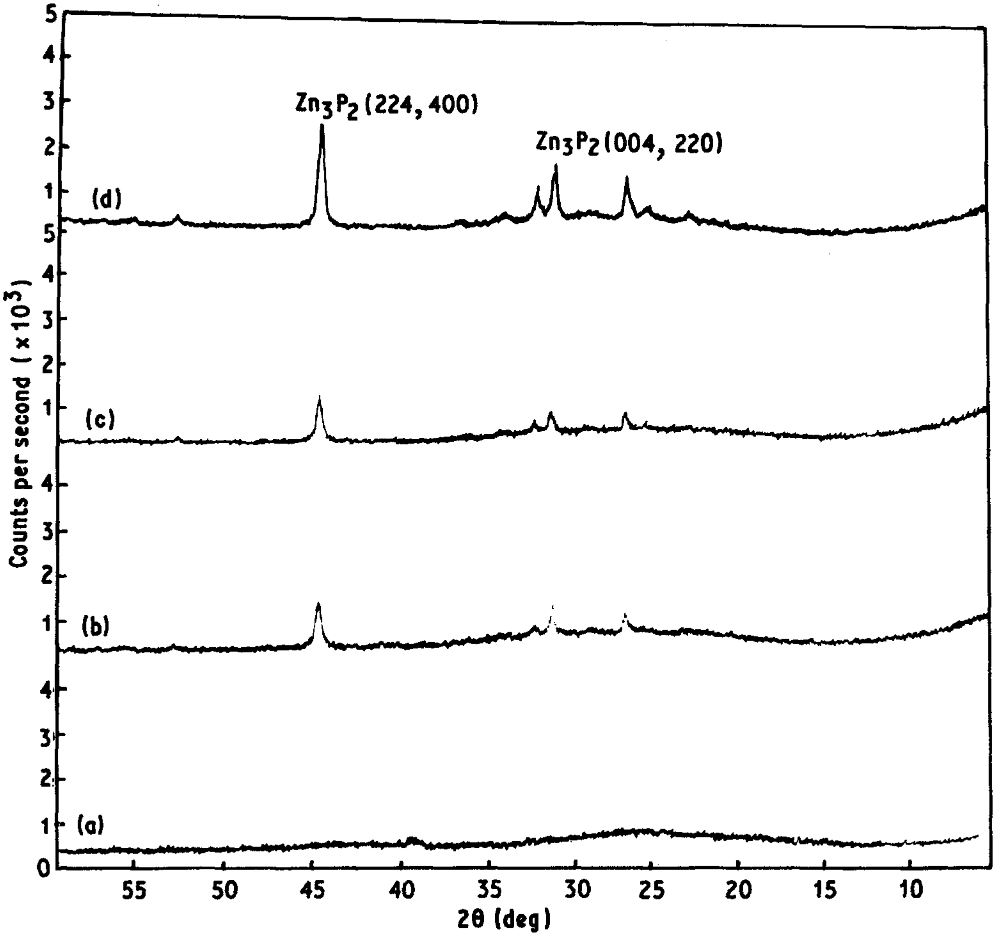

Figure 1 (a) X-ray diffraction spectrum of a Zn_3P_2 film as-deposited on glass and subsequently annealed at 200° C, 250° C and 300° C for 2 h ((b) to (d) respectively).

formed using a Specord UV-VIS double-beam spectrophotometer.

3. Morphology and structure

The XRD results shown in Fig. 1 reveal that the films in their as-deposited condition were non-crystalline. At least, the grain size of the as-deposited films was so small, and the disorder within these grains so great, that no specific diffraction lines could be detected. Comparison of the very broad maxima in Fig. 1 for the as-deposited film with the peaks in Fig. 1 for a fully annealed film shows the existence of a rough correlation of the Bragg angles for the two sets of diffraction patterns, which is anticipated for non-crystalline and crystalline material of the same composition. In Fig. 1, one can observe crystallization to some extent after 2 h anneal at 200 and 250° C and progressively the appearance of a pattern characteristic of well defined crystalline material at 300° C. The sharpening of the peaks observed after an anneal at 300° C for 2 h is indicative of better crystalline order, reduced microstresses and a large grain size, but one may note that after the 250° C anneal (with the exception of two very weak peaks at 23.4° and 25.8°) the remaining peaks are clearly distinguishable. More detailed information about the structural characteristics of the Zn_3P_2 films deposited by electron beam evaporation can be obtained from Table I, when the diffraction peaks obtained from a film annealed at 300° C for 2 h can be compared to those reported from a random powder sample. All of the possibly identifiable diffraction peaks were observed, and matching of the intensities between the two sets of peaks indicates that the annealed film was almost totally free of any preferred orientation, to a degree that rarely occurs in thin films regardless of their mode of deposition.

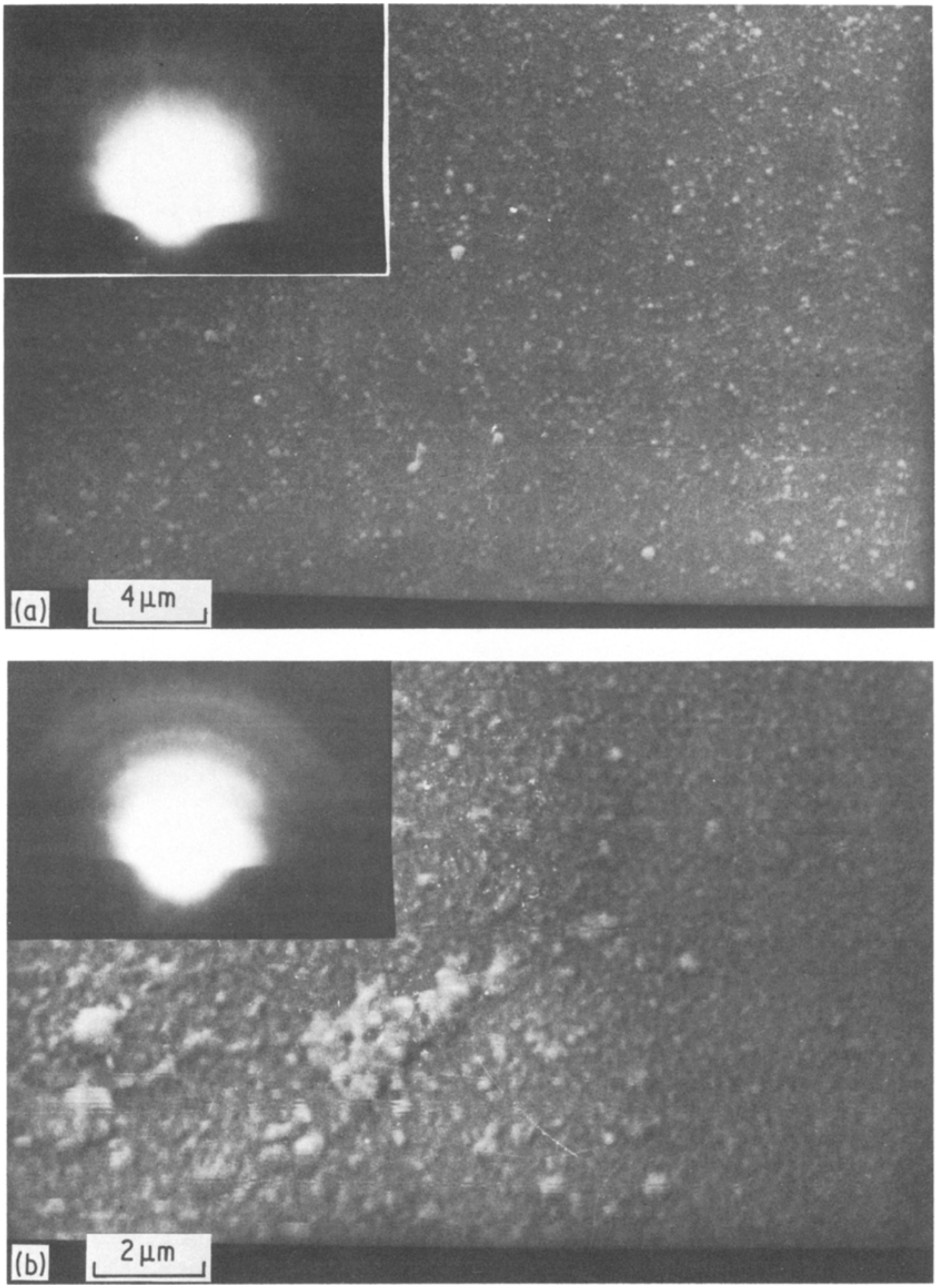

Figure 2 (a) Scanning electron micrograph of unannealed Zn_3P_2 film. (b) Scanning electron micrograph of annealed Zn_3P_2 film.

TABLE I XRD data for Zn_3P_2 (annealed 300° C)

Reported*			Experimental	
d† (nm)	I/I_0	hkl	d (nm)	I/I_0
0.322	50	202	0.329	50
0.285	60	004, 220	0.286	60
0.2010	100	224, 400	0.2017	100
0.1716	50	206, 422	0.1720	50
0.1644	60	404		
0.1424	90	008, 440		
0.1305	50	426, 602		

*ASTM X-Ray Powder Data File, Sets 1–5, Inorganic Volume PD LS 5 iRb, File No. 2-1264, 1960.
†Interplanar spacing (nm).

The X-ray information above is nicely supplemented by the observation made by scanning electron microscopy (SEM) using a Cambridge Stereoscan 150 S. The results are presented in Figs. 2a and b. For the as-deposited sample (Fig. 2a) the SEM micrograph does not reveal any structure, while the electron diffraction pattern, inserted in the upper left-hand corner, shows only the broad halo characteristic of any amorphous material, in agreement with the X-ray results. After 2 h anneal at 200 and 250° C, the results indicate crystallization of a small order corresponding to very faint continuous diffraction rings and the formation of microcrystalline film. Other SEM results not presented here show a continuous transition at temperatures between 200 and 250° C to the structure corresponding to the diffraction pattern characteristic of microcrystalline nature. Fig. 2b shows the SEM micrograph for the film annealed at 300° C for a couple of hours and this indicates crystallinity corresponding to formation of larger grains, which is further confirmed by continuous diffraction rings inserted in Fig. 2b. The micrograph indeed shows that the Zn_3P_2 film is fine-grained with an average size of about 0.8 μm. After crystallization, the films had an essentially random orientation for which evidence can be found in Table I where the intensities of the various XRD peaks for a film annealed at 300° C can be seen to be well correlated to the intensities reported for a powder sample.

4. Optical absorption

Optical absorption spectra are measured at photon energies $h\nu = 1.5$ to 3.2 eV at room temperature. The absorption coefficient is calculated from the measured absorption by means of the relation

$$I = \frac{I_0(1 - R)^2 \exp(-\alpha t)}{1 - R^2 \exp(-2\alpha t)}$$

where t is the sample thickness and R the reflectivity coefficient. The spectral dependence of the absorption coefficient as a function of $h\nu$ was studied for Zn_3P_2 films deposited on glass at room temperature. Fig. 3a shows the absorption

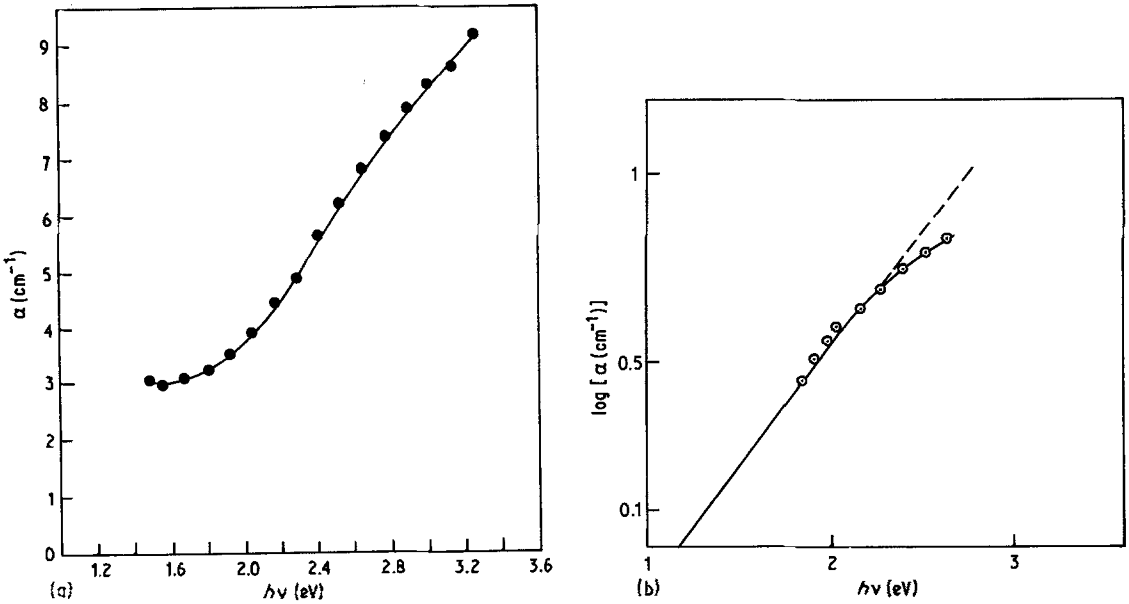

Figure 3 (a) Absorption coefficient of Zn_3P_2 thin film against photon energy (before annealing). (b) Plot of log α against $h\nu$.

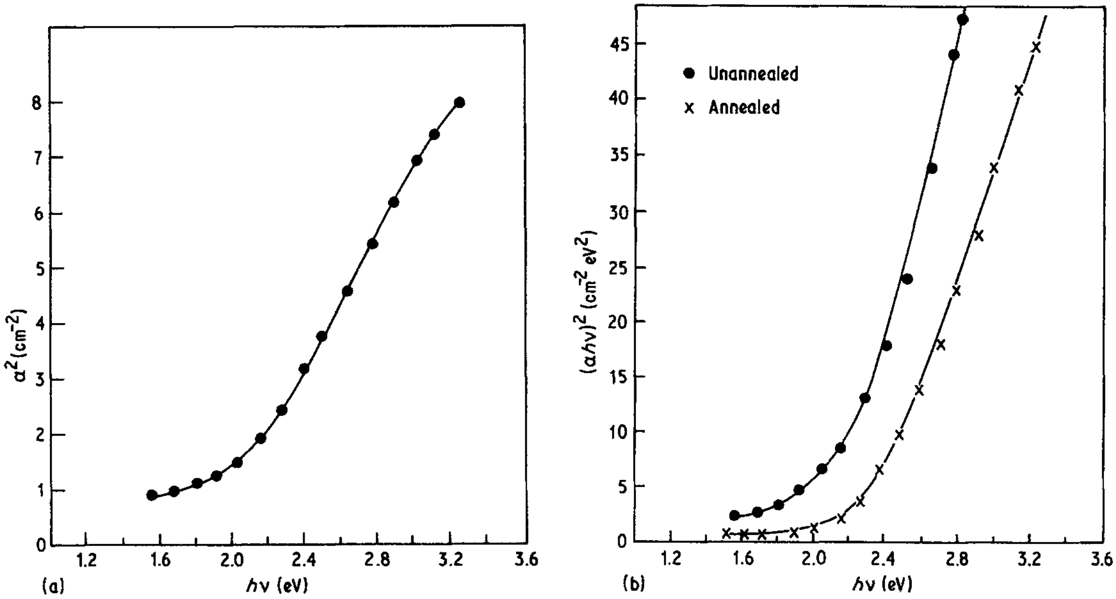

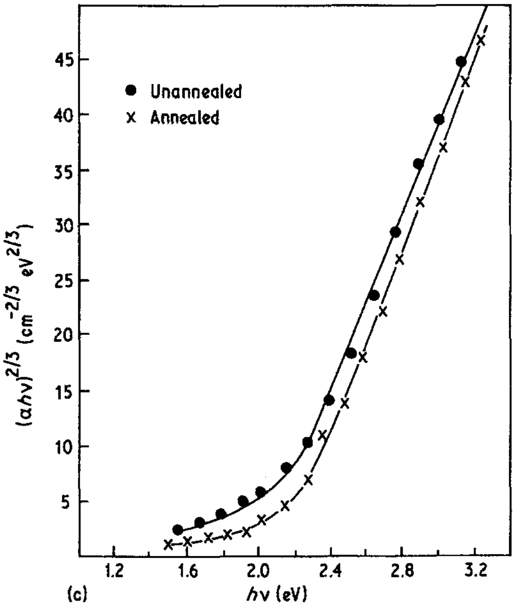

Figure 4 (a) Plot of α^2 against $h\nu$ (unannealed film). (b) Plot of $(\alpha h\nu)^2$ against $h\nu$ (unannealed and annealed film). (c) Plot of $(\alpha h\nu)^{2/3}$ against $h\nu$ (unannealed and annealed film).

plots of amorphous Zn_3P_2 films in the high absorption region. The absorption edge starts sharply at 1.6 eV and there is a strong rise is absorption beginning at 2.02 eV. In view of the broad absorption band, the experimental data near the band edge were analysed in terms of Urbach's relation

$$\alpha = \alpha_0 \exp\left(\frac{-B(h\nu_0 - h\nu)}{kT}\right)$$

where α is the absorption coefficient. The plot of α against $h\nu$ is shown in Fig. 3b. An analysis of the absorption coefficient shows that the rise of α in the energy range $h\nu = 1.5$ to 3.2 eV follows the relation

$$\alpha = \frac{A}{h\nu}(h\nu - E_g)^{1/2}$$

with $E_g = 1.95$ eV (from Figs. 4a and b) which corresponds to an allowed direct transition between parabolic bands. The value of E_g appears to be higher than the reported value of 1.6 eV [10]. This is mainly due to the amorphous nature of the film. A further analysis of the absorption coefficient shows the existence of additional absorption processes. The additional absorption may be due either to a forbidden direct transition or to an indirect transition.

A forbidden direct transition is characterized by

$$\alpha = \frac{A_F}{h\nu}(h\nu - E_{g_F})^{3/2}$$

In Fig. 4c we have therefore plotted $(\alpha h\nu)^{2/3}$ against $h\nu$ to see if this relationship is obeyed. It is seen that a direct forbidden transition (Fig. 4c) is possible with $E_g = 1.99$ eV.

Optical spectra were taken in the same energy range for Zn_3P_2 films annealed at 300° C for 2 h in vacuum. From Figs. 4b and c it is seen that two kinds of transition do occur, namely a direct allowed transition at $E_g = 2.22$ eV and a direct forbidden transition at $E_g = 2.12\,\text{eV}$. On annealing there is a shift in the band edge towards higher energy.

Comparing the values of band gap for sub-microcrystalline (or amorphous) and microcrystalline films we see that for microcrystalline films the band gap is slightly higher.

References

1. A. CATALANO, V. DALAL, W. E. DEVAREY, E. A. FAGEN, R. B. HALL, J. V. MASI, J. D. MEAKIN, G. WARFIELD, N. CONVERSWEJETH and A. M. BARNETT, Proceedings of 13th IEEE Photovoltaic Specialists Conference, 1978, Washington, DC, p. 288.
2. A. CATALANO V. DALAL, Proceedings of the International Conference on Photovoltaic Solar Energy, Luxemburg, 1977 (Reidel, Dordrecht, 1977) p. 644.
3. T. L. CHU, S. CHU, K. MURTHY and E. D. STOKES, *J. Appl. Phys.* **54** (1983) 2063.
4. J. M. PAWLIKOWSKI, *Solid State Electronics* **23** (1980) 755.
5. MADHURI SALVI, V. SAMUEL and V. J. RAO, Proceedings of the Symposium on Photovoltaic Materials and Devices, New Delhi, May 10–11, 1984, p. 89.
6. P. J. LINCHUNG, *Phys. Status Solidi b* **47** (1971) 33.
7. F. C. WANG and R. H. BUBE, *J. Appl. Phys.* **53** (1982) 3335.
8. E. A. FAGEN, *ibid.* **50** (1979) 6505.
9. A. CATALANO, *J. Cryst. Growth* **49** (1980) 681.
10. E. J. JOHNSON, "Semiconductors and semi metals", Vol. III (Academic Press, New York, 1967).

Received 10 July
and accepted 2 November 1984